One Dimensional Local Binary Pattern (LBP) Based EMG Activity Detection for Lower Arm Prosthetics

Paul McCool, Navin Chatlani, Lykourgos Petropoulakis, John J. Soraghan *Senior Member, IEEE*, Radhika Menon and Heba Lakany *Senior Member, IEEE*

***Abstract*— This paper presents a new Electromyography Activity Detection technique in which one-dimensional Local Binary Pattern histograms are used to distinguish between periods of activity and inactivity in myoelectric signals. The algorithm is tested on forearm surface myoelectric signals occurring due to hand gestures. The novel features of the presented method include: a) a simple parameterization approach which provides activity detection across multiple channels without the need for majority vote mechanisms, b) there are no per-channel thresholds to be tuned which makes the process of activity detection easier and simpler to implement and less prone to errors, c) it is not necessary to measure the properties of the signal during a quiescent period before the algorithm can be used. The algorithm is compared to established offline single- and double-threshold activity detection methods and, for the data sets tested, it is shown to have a better overall performance with a lower false positive rate and better tolerance of noisy signals.**

***Index Terms*—1-D Local Binary Patterns, Electromyography activity detection, onset detection, surface electromyography**

I. Introduction

MYOELECTRIC signals have been used for controlling prosthetic hands since the 1960s [1]. The purpose of our work is to develop pattern recognition systems to make myoelectric upper-limb prostheses more useful and intuitive to users [2].

Local Binary Patterns (LBPs) are a powerful texture classification technique for images [3] and video analysis, for example in facial paralysis quantification [4]. LBPs were recently adapted for 1-D signals [5],

Manuscript received 5th August 2013. Part of this work was funded by internal University of Strathclyde research programmes Strathclyde Links and MedTech.

Paul McCool (corresponding author), Lykourgos Petropoulakis and John Soraghan are with the Centre for Excellence in Signal and Image Processing, Department of Electronic and Electrical Engineering, University of Strathclyde, George Street, Glasgow, G1 1XW, UK. (phone: +44-141-548-2935; e-mails {paul.mccool, l.petropoulakis, j.soraghan}@strath.ac.uk).

Navin Chatlani is with Intel Mobile Communications, 1110 American Parkway NE, Allentown, PA 18109 (e-mail: navin.chatlani@gmail.com).

Radhika Menon and Heba Lakany are with the Department of Biomedical Engineering, University of Strathclyde, 106 Rottenrow East, Glasgow, G1 0NW, UK (e-mail radhika.menon28@gmail.com, heba.lakany@strath.ac.uk).

where they were used for Voice Activity Detection. Voiced and unvoiced parts of speech signals were distinguished based on histogram behaviour. We have used LBPs in [6], wherein a novel onset detection technique was described. It takes advantage of the fact that the behaviours of bins in one-dimensional LBP (1-D LBP) histograms differ between periods of Electromyography (EMG) activity and rest. More recently, 1-D LBPs have been used in bone texture characterisation to identify osteoporotic bone structure [7].

This paper targets the onset and activity detection of forearm muscle Surface Electromyography (sEMG) signals. The key advantages of the new technique are:

- It operates on multiple channels to get a single onset/activity decision without the need for setting separate channel thresholds or using majority voting or other techniques to combine separate channel decisions
- It does not require knowledge of the properties (e.g. variance) of a quiescent period or any thresholds defining such a period. Other approaches rely on the assumption that estimates of the noise power can be obtained in this way. Instead, activity/inactivity decisions are made based on the properties of the signal within each window
- There are few parameters to set: Window length/overlap, histogram type and number of histogram bins, which are set only once for a data set with any number of channels

The remainder of the paper is organized as follows: EMG activity and onset detection techniques are described in Section II. Information on myoelectric signals is in Section III. The principles behind 1-D LBP are described in Section IV. In Section V, the proposed 1-D LBP technique for EMG activity detection is presented. The performance evaluation of the technique is given in Section VI. This includes comparisons to other approaches. Conclusions are made in Section VII.

II. Onset and Activity Detection

In pattern recognition for myoelectric signals [8], it is common to infer muscle movement from EMG signals by using onset or activity detection. This is done by measuring when a change in the properties of the signal crosses a threshold. Feature extraction and classification are then performed to interpret the myoelectric signal into finger or hand movement commands for the prosthesis.

A distinction is made in this paper between onset detection and activity detection. Onset detection senses the transition in a signal from 'rest' state to EMG activity. Activity detection identifies and distinguishes between the transitions from rest to EMG activity *and* then back to rest; as such, EMG activity duration is detected. This is useful for control because the prosthesis must respond to stimulus for as long as the user muscle activity is ongoing.

A. Single and double threshold techniques

Methods for onset and activity detection are discussed in [9] [10]. There are two main types: single threshold and double threshold. Single threshold methods allow false alarm probability to be adjusted. One of the simplest onset detection methods, although sensitive to noise, is to measure when the absolute value of the signal is greater than the Root Mean Square plus several standard deviations of a quiescent period of the signal [11].

The Mean Value Comparison method [10] compares the mean of absolute value of windows of the signal to a threshold. Activity is declared for a window if the threshold is exceeded. The energy of the signal can be used to detect onset and activity. In the Short Term Energy method, either the absolute value of the energy in a window must be above a threshold, or the difference in energy between two adjacent windows of the signal must be above a threshold for onset to be declared [8]. This is also simple to implement and can be effective but is sensitive to noise.

In the sliding window average [10] method, the Mean Absolute Value (MAV) of the signal within a window is calculated. Onset is declared at a sample if the MAV goes above a threshold. The Marple-Horvat and Gilbey algorithm [10] detects EMG activity: two adjacent windows are used and the MAV is calculated within each. If the difference of values exceeds or goes below a positive or negative threshold, onset or offset is declared respectively.

Many onset detection methods are based on the properties of the signal envelope. The simplest of these is Differences of Magnitude, which uses the difference in maximum envelope magnitudes between signal windows [9]. The Surf Method detects onset based on the slope of the envelope [9] and is more resilient to

noise. The Fractional Power Envelope method [9] also considers the background noise.

High frequency content method [9] is based on the observation that the high frequency content of myoelectric signals is higher during onset. It detects onsets only.

Double threshold methods allow detection probability to be controlled, in addition to false alarm probability. This is achieved by specifying that a first threshold must be exceeded by a specified number of times (the second threshold) within a window.

The Bonato method is a double-threshold onset detection technique designed for gait analysis [12]. The signal is first whitened, and then a parameter is calculated from two consecutive samples for every odd sample. Onset is declared if the parameter goes above a threshold for a specified number of consecutive times. The probability of detection and probability of false alarm can be separately controlled, but there is a processing overhead when the signal is whitened. Bonato's method includes a postprocessor to remove events of duration ≤30ms.

In Maximum Value Detection [10], the peaks in a window of the signal are counted and onset is declared if the number of peaks exceeds a threshold. Movement can also be detected by measuring the joints of the forearm using sensors such as accelerometers or goniometers. This might be suitable if measuring sEMG from an intact forearm or if there are useable joints on the residual limb of an amputee.

All of the methods discussed here require at least one threshold to be adjusted until the best results are achieved. This is exacerbated if methods are combined or if there are concurrent channels [10], as there are then multiple thresholds to set and co-ordinate.

Another approach is to train a classifier to recognise 'no motion' as a class in the pattern recognition process. If used in a real-time scenario, the classifier is then continuously active and producing class labels, once trained.

In all methods discussed in Section II(A), parameters are calculated and compared against user-defined thresholds, which are decided by comparing characteristics of parts of the signal with and without movement present. A quiescent period of the signal must therefore be identified, which is simple in manual offline analysis but might be difficult to achieve in real-time.

B. Quiescence Detection and Smoothing Filter

The output of onset detection methods is typically an array in computer memory that contains markers at the samples where onsets are detected. Activity detection methods produce an array that contains markers to indicate both onset and subsequent EMG activity. The array is seldom an exact representation of the activity: There can be several markers around an onset and spurious inactivity markers during an active period. To address this, human reaction time period, which is about 300ms [13], can be taken into consideration: all markers in the array that are within this period are assumed to form part of the same intentional movement. Response time is important in upper-limb prostheses, else the user perceives sluggishness [13]. Hence, activity detection, feature extraction and classification must all be calculated within the aforementioned time. Fig. 1 shows the smoothing algorithm used in this work.

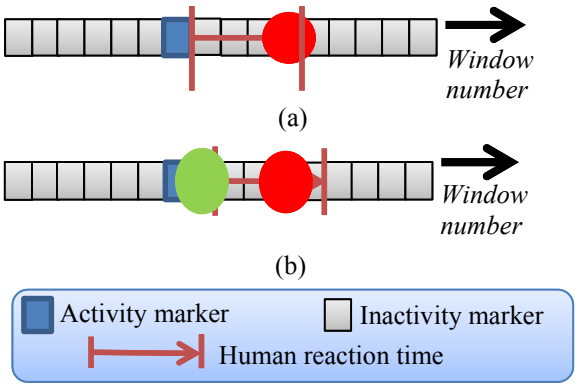

Fig. 1 – Illustration of the smoothing algorithm. (a) Search for activity markers in the array. (b) Set marker (left circled) to 'active', check for more.

'Gaps' between activity markers are 'filled in' if they are within human reaction time of each other as follows:

1. Search sequentially from the start of the array for an activity marker
2. When an activity marker is found, look for at least for one other activity marker within human reaction time of found marker

3. If at least one other marker is found (circled in Fig. 1(a)), set the next marker to 'active' if it is not already (left circled in Fig. 1(b)) and look within human reaction time after that marker (right circled in Fig. 1(b))
4. If no other 'active' maker is found within human reaction time, look sequentially for next 'active' marker and repeat the process

III. The Myoelectric Signal

A. Description

In response to neural drives, electrical fields are generated by propagated action potentials initiated in the muscle fibres of contracting motor units. The summation of the action potential of a single motor unit is the Motor Unit Action Potential (MUAP). The myoelectric signal or surface electromyogram (sEMG) - a measure of this potential - can be expressed as the sum of the attenuated MUAPs with additive noise [14]:

$$x(t) = \sum_j MUAP_j(t) + N(t) \qquad (1)$$

$x(t)$ is the myoelectric signal measured at a single surface site, $MUAP_j(t)$ are the j motor units attenuated by tissue and distance and $N(t)$ is additive noise. Sample rates for sEMG are usually 2-3kHz. Signals are typically band pass filtered between 6-500Hz, because the majority of the sEMG energy is within this bandwidth [15]. The sampled version of the signal is $x[n]$, where n is the sample number.

B. Simulated EMG

Band-limited Gaussian noise can be used as a simulated EMG signal [12] [16] for the purposes of testing onset and activity detection methods. The advantages are that unambiguous onset and offset times can be decided by the experimenter, allowing precise accuracy assessment, and that the SNR can be set by varying the amount of white noise added to the band-passed signal. In this work, the Gaussian noise of sample rate 2kHz was band-limited using an FIR filter with pass band of 6-500Hz. At onset and offsets, the ramped envelope from [16] was used (100 samples) instead of the truncated Gaussian envelope of [12].

C. EMG recordings used in this work

Data Set 1: This data set consists of four gesture classes (tripod, pinch, point, and lateral grip) recorded from three able-bodied volunteers who performed thirty sessions, each consisting of five gestures. The gestures were formed by isotonic muscle contractions and held as isometric contractions for five seconds, with five seconds of rest between each gesture. The gestures were recorded in random sequences. The data set, also used in [6], was recorded in the Department of Biomedical Engineering, University of Strathclyde, UK. All protocols were ethically approved.

Two channels were recorded because most contemporary commercial myoelectric prostheses use two channels. Dry bipolar electrodes (Fig. 2 (a)) were placed on the volunteers' forearms at sites corresponding to the *extensor digitorum* and the *flexor carpi radialis*, which were located using a standard approach [17] [18]. The experiments were conducted with the elbow flexed and forearm in mid-pronation, rested comfortably on a table, with the arm stationary and only the fingers moving to form the gestures (examples in Fig. 2 (b)). The sensors had the same form factor as those used in modern myoelectric limbs, where conducting gel is not used. The sampling frequency (f_s) was 2kHz. The amplifiers, built-in to the sensors, had a high Common Mode Rejection Ratio and a low-pass filter with a cut-off frequency of 500 Hz and a 50Hz notch filter to eliminate power line interference.

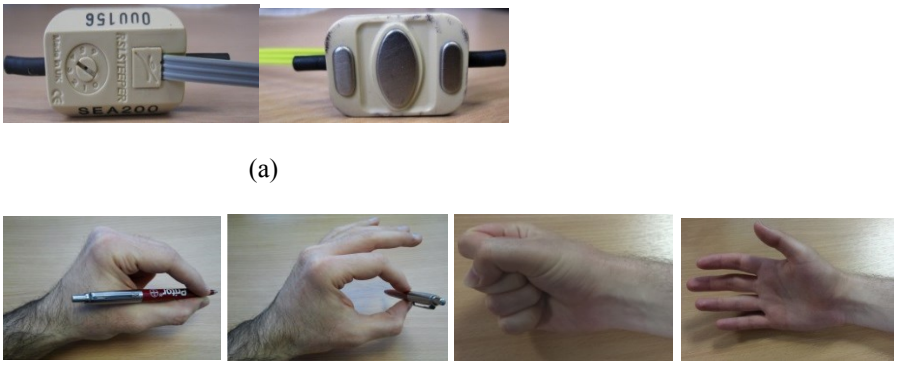

(a)

(b) (c)

Fig. 2. (a) bipolar sensor of the kind used to collect Data Set 1 (b) examples of tripod and pinch gestures from Data Set 1 (c) examples of hand close and hand open gestures from Data Set 2

The movement onset was controlled by displaying visual cues on a screen, and recording the muscle

activity. The volunteers responded to these visual cues, which stated the name and the image of the gesture to adopt (or a 'rest' instruction). In total, about 50% of the data is activity and 50% is rest.

Data Set 2: The data set was recorded from thirty volunteers, with eight channels recorded using bipolar sensors; seven on forearm and one on bicep at a sample rate of 3kHz [19], with a reference Red-Dot electrode on the wrist as ground reference. More details of the electrodes and amplifier can be found in [19]. Seven movement classes (examples in Fig. 2 (c)), wrist pronation/supination, wrist flexion/extension and rest) were recorded. The gestures were performed either from the previous gesture or from rest and then held, corresponding to isotonic followed by isometric muscle contractions, in three second intervals, with five seconds of rest at the start and end of each recording. Each gesture was performed four times per trial in randomized order. The recordings include transitions between gestures, as opposed to returning to rest between every gesture, such that 14.1% of the time between the first and last gestures is rest.

For both data sets, the timestamps of the movement cues had been logged, which formed the 'ground truth' for the comparison among the onset and activity detection algorithms.

IV. One-Dimensional Local Binary Patterns

Two-Dimensional Local Binary Patterns are widely used to extract features from images for texture classification [3]. One-Dimensional Local Binary Patterns (1-D LBPs) are a recent adaptation for one-dimensional signals, in which histograms are generated from data using 1-D LBP codes [5]. The histogram activity is analysed to determine changes in the properties of the signal. In [5], this is used for voice activity detection and to distinguish voiced and unvoiced components. The 1-D LBP code is calculated by comparing the neighbouring samples to sample $x[n]$:

$$LBP_P(x[n]) = \sum_{r=0}^{(P/2)-1} \left\{ S\left[x\left[n+r-\frac{P}{2}\right]-x[n]\right]2^r + S\left[x[n+r+1]-x[n]\right]2^{r+(P/2)} \right\} \quad (2)$$

where $S[.]$ is a threshold function:

$$S[f] = \begin{cases} 1 \text{ for } f \geq 0 \\ 0 \text{ for } f < 0 \end{cases} \quad (3)$$

P is an even number that determines the number of Local Binary Patterns: There are 2^P possible Local Binary Patterns. From (2) and (3), a number, called an LBP code, is derived which reflects the local activity of the signal around a sample relative to its value. The LBP code is thus independent of the absolute amplitude of the signal and of any DC component of the signal. The distribution of LBP codes within a signal (or within a windowed portion of it) is called the LBP histogram [5] and it is calculated as:

$$H_b = \sum_{\frac{P}{2} \leq n \leq N - \frac{P}{2}} \delta(LBP_P(x[n]), b) \quad (4)$$

where H_b is histogram bin number b (each bin corresponds to an LBP code), the signal or windowed portion is of length N, $b = 0..B\text{-}1$, B is the number of histogram bins and $\delta(i, j)$ is the Kronecker Delta.

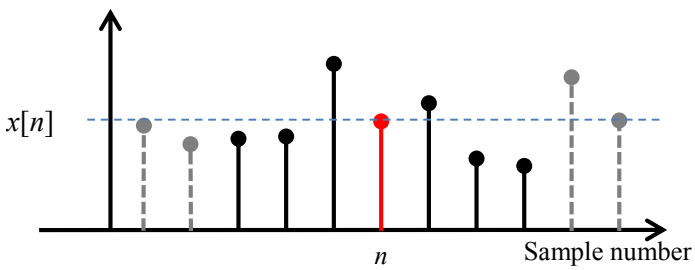

Fig. 3 An example of calculation of an LBP code. The six nearest samples (i.e. $P = 6$) to sample n in signal x are thresholded relative to its value $x[n]$.

Fig. 3 depicts a discrete signal with a sample number n of value $x[n]$. The solid black markers are the six nearest samples to sample n because $P = 6$. The dashed horizontal line shows the value $x[n]$. Of the six samples nearest to n, the two either side of it are greater or equal in value to $x[n]$. Equations (2) and (3) can now be used to calculate the LBP code for sample n. No threshold calculation is performed on sample n, only on the surrounding samples. A worked example is shown in Fig. 4. Note that the least significant bit for LBPs is on the left.

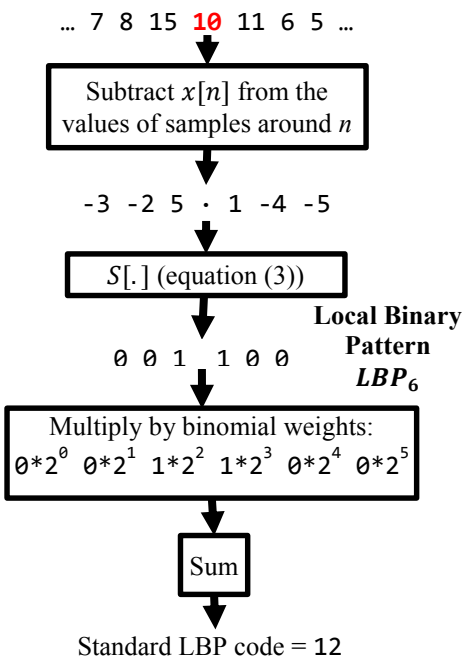

Fig. 4 – Obtaining a 'standard' 1-D LBP code using equations (2) and (3), $P = 6$, $x[n] = 10$

There are three other code types that can be used to form histograms: Uniform, Rotationally Invariant (RI) and Uniform Rotationally Invariant (URI). Uniform histograms have unique bins for each pattern that has at most two 0 to 1 or 1 to 0 transitions. The other patterns are classed as non-uniform and given the same code [3] [5]. Uniform code calculation is shown in Fig. 5.

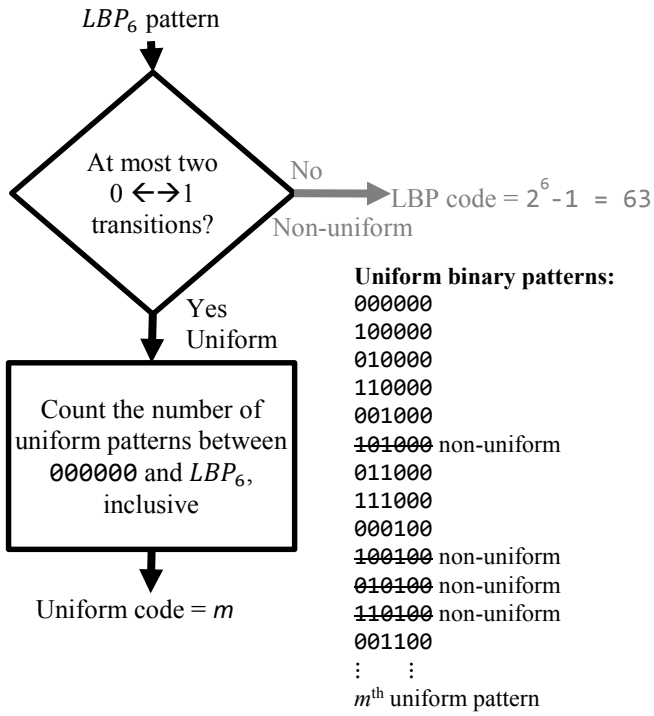

Fig. 5. Calculation of 'Uniform' 1-D LBP code for P=6

Example: Pattern `001100` (in Fig. 4) has 9 uniform binary patterns between `000000` and itself (see right of Fig. 5), so the Uniform LBP code is 8, counting from zero.

To create a Rotationally Invariant LBP, bitwise rotations are performed to minimise the value of the pattern as a binary number, with the least significant bit on the left. This is done using the LBPROT operator, which is adapted from equation (8) in [3] for 1-D LBP:

$$LBP_P^{ri} = \min\{ROL(LBP_P, i) \mid i = 0,1,\dots,P-1\} \qquad (5)$$

where ROL is the binary Rotate Left operator. All rotated versions of the binary pattern are compared, and the version that has the minimum value is taken as the rotationally invariant pattern. In this way, a unique code is created for each rotationally minimum pattern. Fig. 6 shows the process.

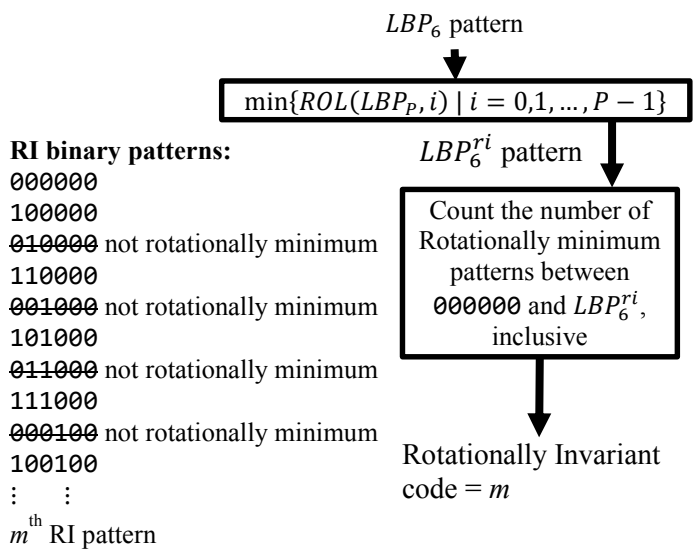

Fig. 6. Flowchart for the calculation of the 'Rotationally Invariant' 1-D LBP code for *P*=6

Example: Pattern `001100` (in Fig. 4) is rotated to the left twice to become `110000`, giving a Rotationally Invariant code of 2 as there are three RI patterns between `000000` and `110000`, counting from zero.

Uniform Rotationally Invariant LBP codes also take into account the transition from the last bit to the first bit when determining uniformity [3]. Fig. 7 shows the process.

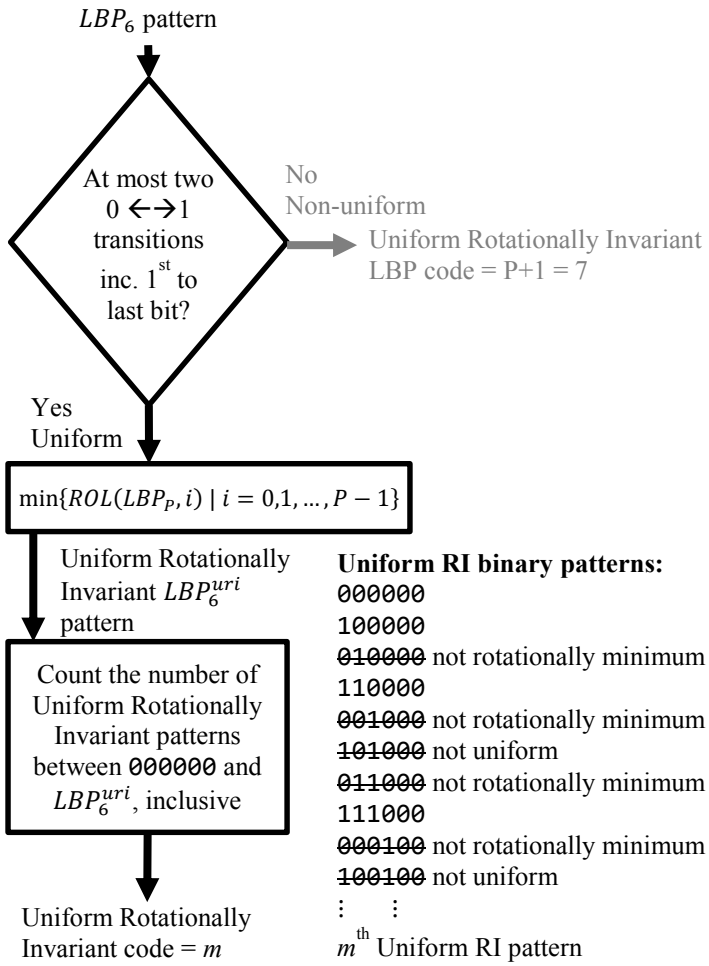

Fig. 7. Flow chart for the calculation of the 'Uniform Rotationally Invariant' 1-D LBP code

Example: Pattern `110001` is rotated left five times to become `111000` giving a Uniform Rotationally Invariant LBP code of 3, counting from zero.

A. Creating a Histogram

Using one of the methods described above, LBP codes are calculated for the signal or window of length N from sample number $(\frac{P}{2}+1)$ to sample number $(N-(\frac{P}{2}+1))$. Once the LBP codes are calculated, a histogram is formed. The total number of histogram bins equals the number of possible unique LBP codes, which depends on the chosen value of P and type of histogram selected.

The number of bins in a rotationally invariant histogram is equal to the total number of unique binary patterns obtainable when each binary number from 0 to 2^P-1 is rotated, by bitwise rotation using (5), to its minimum possible value. The algorithm to generate RI histograms first creates a bin for each unique RI

binary number between 0 to 2^P-1.

V. 1-D LBP FOR EMG ACTIVITY DETECTION

A. 1-D LBP EMG Activity Detection Algorithm

In this section, we show that histograms generated from 1-D Local Binary Patterns can be used on myoelectric signals for EMG activity detection. With 1-D LBP EMG Activity Detection (EAD), the parameters are the window length/overlap, number of histogram bins and the histogram type. The algorithm works based on the observation that the histogram bins behave differently across periods of EMG activity and inactivity.

For EAD, it is necessary to measure the differences between histogram bins within consecutive windows of a signal. It was observed that the normalised amplitude of some histogram bins was greatest when EMG activity is present in a window, and some bins had highest normalised amplitude when there was no EMG activity (i.e. background noise). The amplitudes of these two bin types can be compared directly.

Fig. 8 depicts the stages involved in 1-D LBP EMG Activity Detection (EAD).

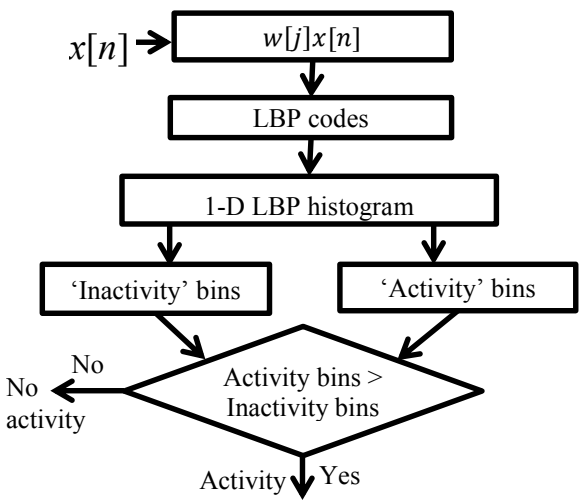

Fig. 8. Flow chart for the One Dimensional LBP EMG Activity Detection (EAD) algorithm

For a single channel:

1. The signal is first split up into windows by applying a window $w[j]$ of length W:

$$x[j] = w[j]x[n] \quad (6)$$

2. Calculate 1-D LBP codes of all the samples in each window using (2) and (3)
3. Calculate standard LBP histogram for each of the windows using (4)
4. Map the standard LBP histogram bins to the histogram bins of the chosen histogram type using (5) and Fig. 5, Fig. 6 and Fig. 7
5. Determine which bins of the histogram correspond to 'activity' and which to 'inactivity' based on Table I.
6. For each window, determine whether the normalised 'activity' bin value is higher than the normalised 'inactivity' bin value
7. Filter the resulting activity vector such that windows with activity detections that are within human reaction time of each other are considered part of the same activity. Use the smoothing algorithm in Fig. 1 for this.

The 'activity' and 'inactivity' bins were identified by observing bin behaviour in real sEMG signals. All of the histogram types were found to have specific bins that were higher in amplitude during quiescent periods and other bins that were higher in amplitude during EMG. From these observations, the formulae to determine the bin numbers were calculated, which are listed in Table I.

TABLE I
LIST OF ACTIVITY BINS AND INACTIVITY BINS FOR EACH HISTOGRAM TYPE FOR EAD

Histogram type	**Total number of bins**	**Activity bin number(s)**		**Inactivity bin number(s)**
Standard	2^P	$2^{(P/2)} - 1$	$2^P - 2^{P/2}$	$2^P - 1$
Uniform	$P(P-1)+3$	$\frac{(7P^2 - 10P + 8)}{8}$	$\frac{-1}{48}P^4 + \frac{13}{24}P^3 - \frac{115}{24}P^2 + \frac{217}{12}P - 20$	$P(P-1)+2$
Rotationally Invariant	Number of unique RI patterns between 0 and 2^P-1	$2^{(P/2)-1}$		*B-1*
Uniform Rotationally Invariant	$P+2$	$P+1$		$P/2$

Note that the 'activity' bin formulae for Uniform histograms in Table I work as high as $P = 10$, which is adequate

for the uses described in this paper. The 'inactivity bin' for all but the Uniform Rotationally Invariant histogram is also the last bin in the histogram. Bin numbering in all cases starts from zero.

B. Testing on a simulated EMG signal

Fig. 9(a) shows a dynamic simulated EMG signal, with a sampling rate of 2kHz and SNR of 6dB. The vertical markers indicate actual onset and offset markers (with 100 sample 'ramps' after each event [16]), and the horizontal line shows the activity estimation by EAD.

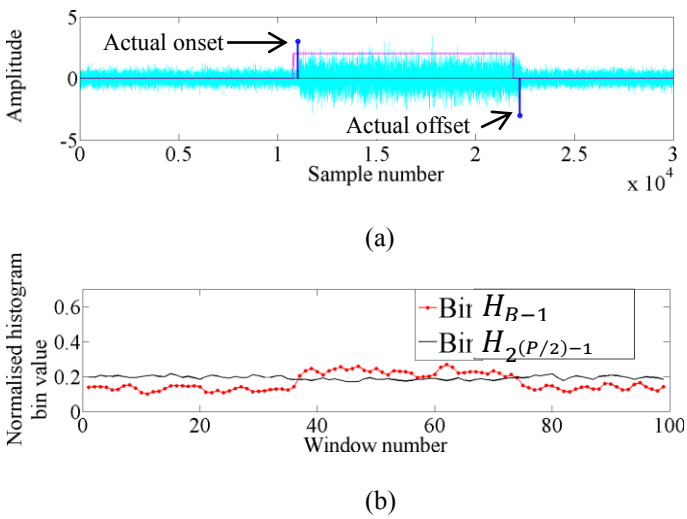

Fig. 9 (a) EAD applied to a dynamic simulated EMG signal of SNR 6dB. (b) Normalized histogram bin activity corresponding to the signal in (a) – dark line is 'inactivity' bin and lighter marked line is the 'activity' bin

Fig. 9 (b) shows the bin behaviour that is used to determine when onset and offset occur: For an RI histogram with P = 4, window size is 600 samples with 50% overlap. During EMG activity, the value in the last bin (H_{B-1}) decreases and the value in bin $H_{2(P/2)-1}$ increases.

Fig. 10(a) shows EAD applied to a single gesture of a real sEMG signal (surface site corresponding to *extensor digitorum* muscle) from Data Set 1. The vertical markers indicate movement and rest cues that were given to the subject. The dashed horizontal line is the activity detection based on the algorithm in Section V A. Fig. 10(b) shows the 'active' and 'inactive' Rotationally Invariant histogram bins (P=4) taken from windows of the signal.

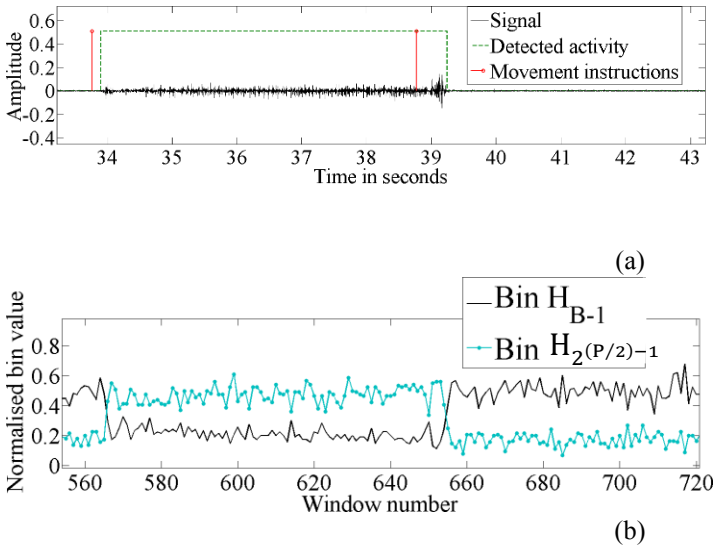

Fig. 10 (a) Surface myoelectric signal from Data Set 1, with activity detection and movement cues superimposed. (b) Normalized histogram bin activity corresponding to the signal in (a) – dark line is RI 'inactivity' bin; marked line is the RI 'activity' bin. Window length is 120 samples with no overlap.

VI. Performance Evaluation

A. Performance measured against other methods

Two separate data sets are used for comparisons. EAD was compared to the Energy activity detection method (energy within a window must be above a threshold) and Bonato's method [12] as explained below. The Bonato method was configured in accordance with the parameters in [16] with the exceptions of *h*, which was varied to make the Receiver Operating Characteristic (ROC) curve. T_1 was set to 1: changing it to 2 or 3 made little difference. Several of the methods described in Section III(A) detect onsets only, so they were not included in this comparative study.

Both channels of Data Set 1 were used together. Bonato's method was applied separately to each channel and activity was declared if at least one channel was active. For Energy, the sum of the energy of both channels within a window had to be above a threshold for activity to be declared. For EAD, a single histogram was created from the LBP codes of both channels together within a window. The Energy and Bonato thresholds were varied to obtain the ROC curves [20]. All sessions of all subjects were used. Adjacent windows of size 60ms (120 samples) with no overlap were used. The resulting curves are shown

in Fig. 11. The quiescent period for Bonato's method was taken as the time between the first two markers ('start of trial' marker and first movement cue).

It was observed that the time between a movement cue and EMG activity for all subjects in Data Set 1 was typically about 200ms. This value was therefore taken as the reaction time throughout this experiment: EMG onsets and offsets were assumed to be consistently 200ms after the movement and rest cues. All the activity detection methods were compared against this. To investigate the consistency of this standard, different assumptions about the delays were tested: Using 180ms and 220ms assumptions respectively slightly deteriorated and improved the results for all methods. Consequently, a value of 200ms for the reaction time was considered to be appropriate for Data Set 1.

It is necessary to create a reference template, or 'gold standard', against which activity detection methods can be compared for each trial in the data sets. For this, the movement cues that were recorded with the data sets were used along with the assumption about reaction times discussed above. For an EMG recording session, an 'activity/inactivity' array is made, which is the same length as the recording, where '1' represents activity and '0' represents inactivity' for each sample of the recording. The activity detectors were programmed to produce this same format of output, so that a direct comparison can be made. This way, True Positive Rate (TPR), False Positive Rate (FPR) [20] and accuracy can all be calculated on a sample-by-sample basis.

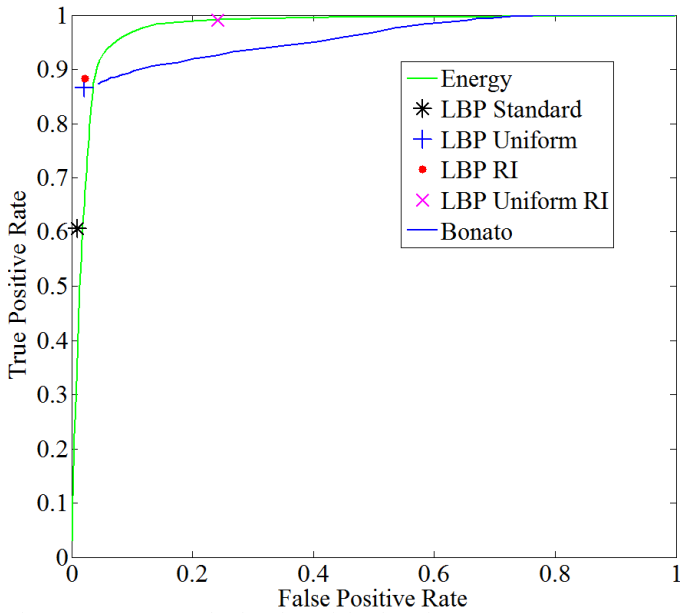

Fig. 11 ROC curves and points for activity detection on Data Set 1. Energy, Bonato (T_1 = 1) and EAD (P = 4). Window length 120 samples (60ms) with no overlap and 200ms smoothing window for both Energy and EAD

Fig. 11 shows ROC curves for the Energy and Bonato methods and symbols to represent the markers for each of the four LBP histogram types where there are no ROC curves since there are no manual thresholds to sweep. ROC curves are direct indicators of performance (accuracy and robustness), with the target being simultaneous maximization of TPR and minimization of FPR values and they help obtain near optimal designs. Figure 11 shows that superior TPR and FPR values are possible using LBP with P=4 (chosen experimentally) compared to both the Energy and Bonato methods, for this data set, when using the combined results for all three subjects. For each subject individually, the TPR/FPR achieved was better than or similar to the results for Energy and Bonato's method.

The much noisier Data Set 2 was used for a comparison between the two algorithms that gave the best results for Data Set 1: Energy and EAD. The Bonato method would have required a subjective majority vote system across all eight channels and did not perform as well on Data Set 1.

The results from all thirty subjects were used and the mean values of the combined results were plotted for comparison (Fig. 12). For EAD, the window length was 300ms with 50% overlap for all trials and subjects, with P set to 4. Energy's performance was better with 60ms windows, which was used. The human reaction time was assumed to be 300ms for this data set, so this was used as the duration of the smoothing

filter. The markers indicate the mean TPRs and FPRs for the histogram types and the line is mean energy ROC across all thirty subjects, obtained by averaging the TPR for FPRs at twenty points across the FPR axis. The superior EAD performance is evident: the Standard histogram has lower FPR for the same TPR compared to the Energy method.

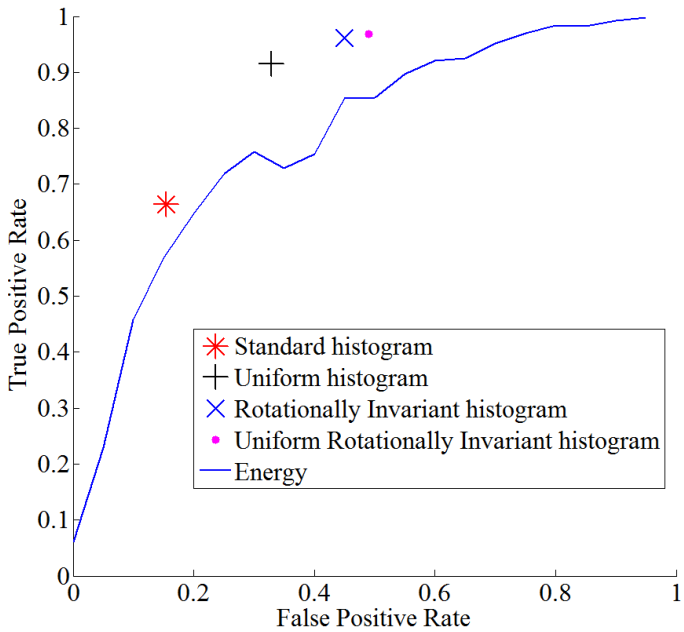

Fig. 12 ROC depicting a comparison between Energy and EAD combined results from all subjects in Data Set 2. $P = 4$, window length 60ms for Energy and 300ms with 50% overlap for EAD

B. Comparison with classifiers trained to recognize 'no motion' class

EAD was also compared with classifiers that were trained to recognize 'motion/no motion' classes. Data Set 1 was used. A Linear Discriminant Analysis (LDA), a Neural Network and a 1v1 Support Vector Machine (SVM) were tested. The mean of the accuracy, TPR and FPR were determined for the three subjects of the data set. The results are shown in Table II.

TABLE II

COMPARISON OF EAD WITH CLASSIFIERS, WINDOW LENGTH 60 MILLISECONDS USING ALL SUBJECTS OF DATA SET 1, TWO CHANNELS OF HUDGINS' TIME DOMAIN FEATURE SET [21], 40 WINDOWS TAKEN 200MS AFTER MOVEMENT/REST CUE, 60MS WINDOWS WITH 30MS OVERLAP, 60/40 TRAINING/TEST RATIO

Method	Accuracy %	TPR	FPR
EAD, both channels (RI *P*=4)	93.9	0.8829	0.0216
Linear Discriminant	88.2	0.89	0.08
Linear Support Vector Machine	89.5	0.83	0.04
NN (3 runs per subject)	92.9	0.92	0.06
NN with PCA preprocessing (3 runs per subject)	93.2	0.92	0.05

In this case, the neural network had similar accuracy, better TPR, but worse FPR than EAD. In practical prostheses applications, consistency and robustness are important, so superior FPR performance is preferable to avoid unintentional movement, whereas prosthetic users can compensate for a lower TPR by retrying. Moreover, the statistical nature of neural network training means that the results were not consistent between runs, unlike EAD.

C. Comparison between 1-D LBP histogram types for activity detection

The performances of the histogram types were tested across all of Data Set 1 and results are shown in Table III.

TABLE III

COMPARISON BETWEEN HISTOGRAM TYPES FOR ACTIVITY DETECTION ACROSS DATA SET 1, *P*=4, WINDOW LENGTH 60 MILLISECONDS

Histogram type	Accuracy (%)	TPR	FPR	SD
Standard	83.3	0.6071	0.0098	0.1
Uniform	93.3	0.8661	0.0203	0.0501
Rotationally Invariant	**93.9**	**0.8829**	**0.0216**	**0.0476**
Uniform Rotationally Invariant	85.4	0.9903	0.2414	0.0706

Table III shows a comparison of the different histogram types and their performance in the activity detection algorithm. The Rotationally Invariant and the Uniform Histograms can be seen to have the best balance between accuracy, TPR and FPR with little difference between them for Data Set 1. The parameters should be chosen experimentally for a given data set and with the SNR taken into consideration.

TABLE IV

COMPARISON BETWEEN VALUES OF *P* FOR ROTATIONALLY INVARIANT HISTOGRAM ACROSS DATA SET 1, WINDOW LENGTH 60 MILLISECONDS

P	Accuracy (%)	TPR	FPR
2	93.9	0.8852	0.0232
4	93.9	0.8829	0.0216
6	92.2	0.8374	0.0187
8	89.1	0.7562	0.0159
10	83	0.6042	0.0124

Table IV shows the accuracies, TPR and FPR for different values of *P* across all of Data Set 1. An RI histogram and window length of 60ms (120 samples) were used. The smoothing algorithm was used with length 200ms. It can be seen that *P*=2 and *P*=4 produce similar results with this data set.

D. Effects of varying the window length and overlap

The window length and overlap affect the responsiveness of detection. An activity decision is made by the algorithm for every interval equal in duration to window length minus any overlap. It is generally necessary to use longer windows for lower SNRs, so increasing the overlap improves the responsiveness. However, using very short windows was found experimentally to increase the FPR. Table V shows that the accuracy does not vary significantly for window lengths above about 50ms for Data Set 1.

TABLE V

ACCURACIES OBTAINED BY VARYING THE WINDOW LENGTH ACROSS DATA SET 1 USING EAD, ROTATIONALLY INVARIANT HISTOGRAM, *P*=4

Window length (ms)	Accuracy (%)	TPR	FPR
5	76.34	0.9951	0.3979
10	93.79	0.9729	0.0865
25	95.1	0.9250	0.0303
50	94.2	0.8922	0.0229
75	93.8	0.8799	0.0214
100	93.5	0.8714	0.0199
250	92.9	0.8554	0.02
500	92.3	0.844	0.0217
1000	90.6	0.8129	0.0287

The window length determines the smoothness of the activity detection, but as window length increases, resolution decreases. The use of overlapping windows was found to mitigate this. Degrees of overlap were compared for a fixed window length. The results in Table VI indicate that adjusting the overlap improves

the FPR slightly but does little to improve the accuracy for Data Set 1.

TABLE VI

ACCURACIES OBTAINED BY VARYING THE AMOUNT OF WINDOW OVERLAP ACROSS DATA SET 1 USING EAD, WINDOW LENGTH 60 MILLISECONDS, ROTATIONALLY INVARIANT HISTOGRAM, P=4

Overlap (%)	Accuracy (%)	TPR	FPR
0	93.92	0.8829	0.0216
25	93.8	0.8793	0.0211
50	93.69	0.8759	0.0206
75	93.15	0.8615	0.0198
90	92.87	0.8541	0.0194

The length of a window and the overlap are decided by:

- SNR – based on tests with simulated EMG, lower SNRs require longer window lengths
- Desired resolution of activity detection
- Desired smoothness of activity detection
- Value of P: in general, higher values of P should be used for lower SNRs

The EAD algorithm does not detect transitions between non-rest gestures; transitions to and from rest are identified.

E. Discussion

From Table III, it can be seen that the best histogram types for activity detection are Rotationally Invariant and Uniform. The Uniform histogram was also found experimentally to be useful when testing on noisier simulated data. The Uniform Rotationally Invariant method was the most sensitive; it had a higher FPR than the other histogram types, especially if the data was noisy, so may therefore not be as useful as an activity detector unless it can be improved by post-processing.

EAD is easily set up and provides good activity detection performance with few parameters to adjust irrespective of number of channels used – unlike other methods where individual channel tuning and additional processing are necessary. EAD could therefore provide a means to obtain quick and quite accurate results by which other methods can be compared.

In all the cases studied, choosing window length, P (therefore the number of histogram bins) and

histogram type to obtain the best accuracy depends on the SNR. For example, for Data Set 1, due to the high SNR, a lower value of *P*, shorter window length and RI histogram were found to be more appropriate.

With multiple channel outputs, fair comparisons with methods, primarily developed for individual channel use, are not easy. In the case of Bonato, a comparison for eight channels would have required a subjective majority vote approach.

Both Energy and EAD algorithms had lower performance with the noisy Data Set 2, but EAD displayed more robustness even though the parameters were not separately adjusted to get the best results for each of the 240 trials that were used.

VII. Conclusion

This paper has presented a novel multi-channel EMG activity detection algorithm, which uses histograms obtained from the recently-developed one-dimensional local binary pattern method. The algorithm has a few parameters to set: window length/overlap, histogram type and the number of histogram bins. These are set once for an entire data set, and for the data sets used, results rivalling or improving on those of the Energy and Bonato methods were obtained.

The notable advantages of the proposed method are that a single activity/inactivity decision is given for multiple channels with few tuning parameters. The process requires no preprocessing such as whitening. For multiple concurrent EMG channels, the LBP codes, across the concurrent window of each channel, are simply amalgamated into a single histogram, rather than requiring a, usually subjective, Majority Vote mechanism. Increased robustness has also been demonstrated both in terms of lower FPR and in the presence of noisy signals.

In future work, real-time testing would assess the applicability of the algorithm for use in prostheses as SNR changes. Fitting currently available commercial myoelectric prosthetic hands to patients requires manual calibration of threshold settings by clinicians according to each patient's ability. It is common for patients to return to the clinic for threshold values readjustment because conditions change such as muscle tone and sensor slippage. Therefore, the amount of noise during inactivity and the signal to noise ratio

(SNR) changes[1]. In future work, we will investigate the benefits of EAD to reduce the need for recalibration.

EAD has not been tested on recordings of slow, intentional movements. The possibility of modifying the algorithm to detect changes between gestures without going through 'rest' first will be investigated. Future work will also investigate the real-time performance of the algorithm.

ACKNOWLEDGMENT

The authors would like to thank Touch EMAS for providing the sEMG sensors to record Data Set 1. The authors thank Professor Adrian Chan from Carleton University, Canada, for providing Data Set 2 [19].

REFERENCES

[1] E. David Sherman, "A Russian bioelectric-controlled prosthesis", Canada Med. Ass. Journal, pp. 1268-1270, 12 Dec 1964.

[2] Silcox DH 3rd, Rooks MD, Vogel RR, Fleming LL., "Myoelectric prostheses. A long-term follow-up and a study of the use of alternate prostheses", The Journal of Bone and Joint Surgery American volume, 75(12), pp. 1781-9, Dec 1993.

[3] Timo Ojala, Matti Pietikäinen, and Topi Mäenpää, "Multiresolution gray-scale and rotation invariant texture classification with Local Binary Patterns", IEEE Transactions On Pattern Analysis And Machine Intelligence, Vol. 24, No. 7, July pp. 971-987, 2002.

[4] Shu He, John J. Soraghan, Brian F. O'Reilly and Dongshan Xing, "Quantitative analysis of facial paralysis using Local Binary Patterns in biomedical videos", IEEE Transactions on Biomedical Engineering, Vol. 56, NO. 7, July 2009.

[5] N. Chatlani and J. Soraghan, "Local Binary Patterns for 1-D signal processing", 18th European Signal Processing Conference (EUSIPCO 2010), pp. 95-99, 23-27 August 2010.

[6] P. McCool, N. Chatlani, L. Petropoulakis, J. J. Soraghan, R. Menon, H. Lakany, "1-D Local Binary Patterns for onset detection of myoelectric signals", EUSIPCO 2012.

[7] Lotfi Houam, Adel Hafiane, Abdelhani Boukrouche, Eric Lespessailles, Rachid Jennane, "One dimensional local binary pattern for bone texture characterization", Springer-Verlag, Pattern Anal Applic, pp. 1-15, 7 Sep 2012.

[8] B. Hudgins, P. A. Parker, "A New Strategy For Multifunction Myoelectric Control", IEEE Trans. On Biomedical Engineering, Vol. 40, No.1, January 1993.

[9] Jian-Jiun Ding , Chi-Jung Tseng , Che-Ming Hu, and Ta Hsien, "Improved onset detection algorithm based on fractional power envelope match filter", 19th European Signal Processing Conference (EUSIPCO 2011) Barcelona, Spain, August 29 - September 2, 2011.

[10] Sun Qizhu, Sun Yining and Ding Xiangfeng, "Onset determination of muscle contraction in surface electromyography signals analysis", 2005 IEEE, International Conference on Information Acquisition, June 27 - July 3, 2005, Hong Kong and Macau, China.

[11] S. Micera, G. Vannozzi, A. M. Sabatini, P. Dario, "Improving detection of muscle activation intervals", IEEE Engineering in Medicine and Biology, November/December 2001.

[1] Based on discussion with Touch EMAS

[12] Paolo Bonato, Tommaso D'Alessio and Marco Knaflitz, "A statistical method for the measurement of muscle activation intervals from surface myoelectric signal during gait", IEEE Transactions on Biomedical Engineering, Vol. 45, No. 3, March 1998.

[13] Kevin Englehart and Bernard Hudgins, "A Robust, Real-Time Control Scheme for Myoelectric Control", IEEE Trans. Biomed. Eng, 50 (7), pp. 848-854.

[14] A. Merlo, D. Farina, R. Merletti, "A fast and reliable technique for muscle activity detection from surface EMG signals", IEEE Trans. Biomed. , Eng. 50 (3) (2003), pp. 316–323.

[15] Peter Konrad, "The ABC of EMG – A practical introduction to kinesiological electromyography", Version 1.0, April 2005

[16] Gerhard Staude, Claus Flachenecker, Martin Daumer, Werner Wolf, "Onset Detection in Surface Electromyographic Signals: A Systematic Comparison of Methods", EURASIP Journal on Applied Signal Processing 2001:2, pp. 67– 81.

[17] Pease, W.S., Lew, H.L., Johnson, E.W., Johnson's Practical Electromyography, 4th Ed., Lippincott Williams & Wilkins, 2006

[18] Jennifer Chu-Andrews and Robert Joseph Johnson, "Electrodiagnosis: An Anatomical and Clinical Approach", 1986, ISBN 0397506872

[19] A. D. C Chan and G. C. Green, "Myoelectric control development toolbox," presented at the 30th Conf. Can. Med. Biol. Eng. Soc., Toronto, Canada, 2007, Paper M0100.

[20] 1. Zweig, MH, Campbell, G., "Receiver-operating characteristic (ROC) plots: A fundamental evaluation tool in clinical medicine", Clin Chem 1993;39/4, 56-577.

[21] K. Englehart, B. Hudgins, P.A. Parker and M. Stevenson, "Classification of the Myoelectric Signal using Time-Frequency Based Representations", Medical engineering and physics 21, no. 6 (1999): 431-438.

Paul McCool received B.Eng. (Hons.) degree in electronic engineering and physics from the University of Glasgow, UK, in 1999, and M.Sc. (with distinction) in electronic and electrical engineering from the University of Strathclyde, Glasgow, UK, in 2010.

He worked as a Project Officer in the Defence Equipment and Support agency of the UK Ministry of Defence between 1999 and 2009. He is currently a PhD Student at the University of Strathclyde, Glasgow, UK, researching pattern recognition and muscle activity detection for forearm myoelectric signals to control a prosthetic hand.

Mr McCool is a member of the IET.

Navin Chatlani received the B.Sc. (Hons.) degree in electrical and computer engineering from the University of the West Indies, Trinidad, in 2002 and the M.Sc. (with distinction) and Ph.D. degrees in electronic and electrical engineering from the University of Strathclyde, Glasgow, U.K., in 2007 and 2011, respectively. His doctoral research focused on advanced signal enhancement techniques with application to speech and hearing.

From October 2010 to March 2012 he has was a Postdoctoral Research Fellow at the Centre for Excellence in Signal and Image Processing, University of Strathclyde, investigating methods for noise reduction, voice activity detection, beamforming, and event onset detection. Currently he works with the Audio R&D team at Intel Mobile Communications developing novel techniques for speech processing technologies. His main research interests are signal processing theories, algorithms, architectures, and filtering techniques for speech/audio applications and biomedical data applications.

Lykourgos Petropoulakis obtained a 1st class BSc degree in Aeronautical Engineering and a PhD in Control Engineering from the University of Salford, UK. Subsequently, he joined Edinburgh University where he worked as a researcher in artificial intelligence and robotics. In 1992 he accepted a lectureship position in the Department of Electronic and Electrical Engineering in the University of Strathclyde. Dr. Petropoulakis has over 40 publications in journals and conferences. His current interests are in robotics, microprocessors, prosthetic devices, intelligent systems and bioengineering.

John J. Soraghan (S'83–M'84–SM'96) received the B.Eng. (Hons.) and M.Eng.Sc. degrees in electronic engineering from University College Dublin, Dublin, Ireland, in 1978 and 1983, respectively, and the Ph.D. degree in electronic engineering from the University of Southampton, Southampton, UK, in 1989. His doctoral research focused on synthetic aperture radar processing on the distributed array processor.

He was a Manager of the Scottish Transputer Centre from 1988 to 1991, Manager with the DTI Parallel Signal Processing Centre from 1991 to 1995 and Head of the ICSP from 2005-2007. He currently holds the Texas Instruments Chair in signal processing within the Centre for excellence in Signal and Image Processing (CeSIP), University of Strathclyde. His main research interests are signal processing theories, algorithms, and architectures with applications to high resolution methods for radar and acoustics, biomedical data processing, video analytics for surveillance, 3D video and condition monitoring. Professor Soraghan is a member of the IEEE Signal Processing in Education Technical Committee, a Member of the IET and a Senior Member of the IEEE.

Radhika Menon received a 1st class BTech degree in Electronics and Communication Engineering from the National Institute of Technology, Warangal, India, in 2008. Thereafter she worked as a Software Engineer in Samsung Software Operations, Bangalore, India, until 2010. She

completed M.Sc. (with distinction) in Bioengineering in 2011 at the University of Strathclyde, Glasgow, UK, where she worked as a Research Assistant until April 2012. Her work involved surface EMG data acquisition and signal processing of EMG data for pattern recognition for hand gestures. She is also interested in virtual reality simulators used in Rehabilitation Engineering.

Heba Lakany received PhD in Artificial intelligence from the University of Edinburgh in 1999. She is currently a lecturer at the Department of Biomedical Engineering, University of Strathclyde, Scotland. Prior to this, she had been a lecturer in the department of Computer Science at the University of Essex (2001-2007) and a Research Fellow in the Centre of Brain Research, Department of Medical Physics and Medical Engineering of the University of Edinburgh (1999-2001). Dr Lakany is a Senior Member of the IEEE and a fellow of the Academy of Higher Education (UK).

Her research interests include applications of pattern recognition and artificial intelligence techniques in rehabilitation engineering, motor control and neuroprosthetics.